International Journal of Nanomedicine Dovepress

Open Access Full Text Article ORIGINAL RESEARCH

Curcumin-Loaded Gelatin Nanoparticles Cross the Blood-Brain Barrier to Treat Ischemic Stroke by Attenuating Oxidative Stress and Neuroinflammation

Qinglu Yang[1,*], Ruitong Li[2,*], Yigen Hong[1], Hongsheng Liu[3], Chuyao Jian[1], Shaofeng Zhao[1]

[1]Department of Rehabilitation Medicine, The Eighth Affiliated Hospital of Sun Yat-Sen University, Shenzhen, Guangdong, People's Republic of China; [2]Department of Psychology and Human Development, IOE, UCL's Faculty of Education and Society, University College London, London, WC1H 0AL, UK; [3]Guangdong Huayi Biomedical Science and Technology Center, Guangzhou, Guangdong, People's Republic of China

*These authors contributed equally to this work

Correspondence: Chuyao Jian; Shaofeng Zhao, Email jianchy3@mail.sysu.edu.cn; shaofengzhao88@163.com

Background: Ischemic stroke is a medical emergency for which effective treatment remains inadequate. Curcumin (Cur) is a natural polyphenolic compound that is regarded as a potent neuroprotective agent. Compared to synthetic pharmaceuticals, Cur possesses minimal side effects and exhibits multiple mechanisms of action, offering significant advantages in the treatment of ischemic stroke. However, drawbacks such as poor water solubility and transmembrane permeability limit the efficacy of Cur. In recent years, nano-delivery systems have attracted great interest in the field of stroke therapy as an effective method to improve drug solubility and cross the blood-brain barrier (BBB).

Methods: In this study, a novel nanomedicine (Cur@GAR NPs) for ischemic stroke treatment was developed based on Cur-loaded gelatin nanoparticles (Cur@Gel NPs) that were then functionalized and modified with rabies virus glycoprotein (RVG29) to target brain tissue. The stability, antimicrobial properties, antioxidant properties, neuroprotective effects, neuronal cell uptake, and biocompatibility of Cur@GAR NPs were investigated in vitro. The in vivo therapeutic effect of Cur@GAR NPs on ischemic stroke was investigated in a middle cerebral artery occlusion (MCAO) rat model using the Morris water maze test and the open field test, and the potential mechanism of action was further investigated by histological analysis.

Results: The resulting Cur@GAR NPs improved the solubility of Cur and exhibited good dispersion. In vitro studies have shown that Cur@GAR NPs exhibit great antimicrobial properties, antioxidant properties and intracellular reactive oxygen species (ROS) protection. Notably, RVG29 significantly enhanced the uptake of Cur@GAR NPs by SH-SY5Y cells. Furthermore, in vivo studies verified the role of Cur@GAR NPs in reducing nerve damage and supporting neurological recovery. In the MCAO rat model, Cur@GAR NPs significantly attenuated neuroinflammation, reduced neuronal apoptosis and restored behavioral functions to a great extent.

Conclusion: Together these findings implied that Cur@GAR NPs could provide a novel and promising approach for effective ischemic stroke treatment.

Keywords: ischemic stroke, nanomedicine, anti-inflammatory, antioxidant, targeted delivery

Introduction

Stroke is a severe medical emergency caused by an interruption or blockage of the blood supply to a specific area of the brain.[1] Ischemic stroke is the most common type of stroke and poses a significant risk of mortality and disability.[2–4] When blood flow to the brain is suddenly interrupted, nerve cells are rapidly affected by hypoxia and nutrient deficiency, resulting in ischemic injury. Ischemic injury triggers microglia in the brain to convert to a pro-inflammatory phenotype, producing large amounts of inflammatory mediators. These inflammatory mediators further recruit and activate peripheral

Received: 3 September 2024
Accepted: 5 November 2024
Published: 10 November 2024

Graphical Abstract

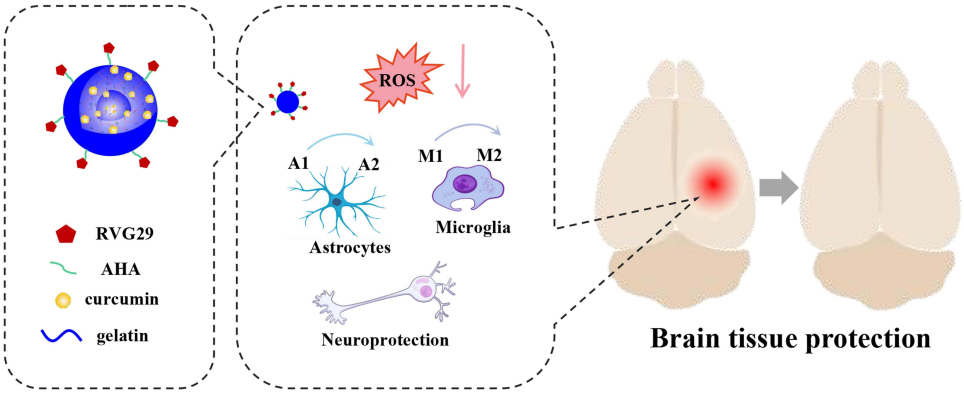

immune cells, exacerbating the inflammatory response. In addition, insufficient intracellular oxygen supply during ischemia leads to mitochondrial dysfunction, metabolic disturbances, and energy depletion. When blood flow is reperfused, the sudden increase in oxygen leads to the production of large amounts of reactive oxygen radicals (ROS), resulting in oxidative stress. Neuroinflammation and oxidative stress mutually promote and amplify each other, establishing a vicious cycle that precipitates neuronal injury and death.[5–7] Currently, thrombolysis and neuroprotection are the two main therapeutic options for ischemic stroke intervention.[8] However, there is still no effective treatment for ischemic stroke due to limitations such as a narrow therapeutic window, low success rate of single-agent therapy, systemic toxicity, and BBB impediments to drug delivery.[9–11] As such, it is imperative to develop new therapeutic strategies for treating ischemic stroke.

Prior research has demonstrated that numerous active ingredients extracted from traditional herbs exhibit protective effects against ischemic stroke with minimal side effects.[12–16] Natural drug molecules thus hold great promise in the development of innovative multi-target drugs for stroke treatment. Cur is a natural polyphenolic compound with a wide range of biological activities.[17,18] Studies have shown that Cur has favourable pleiotropic effects in neuroprotection, including anti-inflammatory, antioxidant, antitau hyperphosphorylation, anti-amyloid, and metal chelating activities.[19,20] Nevertheless, Cur and its derivatives exhibit restricted therapeutic efficacy, primarily attributed to challenges like low water solubility, short half-life, inadequate transmembrane permeability, vulnerability to degradation, and poor bioavailability.[21] Nanotechnology-based delivery systems are an effective and promising approach to alleviate drug problems associated with Cur delivery.[22,23]

Recently, nanomedicines have garnered considerable interest as an emerging and effective therapeutic approach in stroke treatment.[2] In comparison to traditional drugs, nanomedicines offer the benefits of enhancing drug stability, facilitating easy modification, controlling the rate of drug release, enhancing the permeability of biological membranes, prolonging the duration of action, and reducing the frequency of drug administration.[24,25] Importantly, the BBB, a unique physiological barrier of the brain that restricts the entry of all macromolecules and 98% of small molecule drugs into the brain, poses a major difficulty in the treatment of brain injury.[26,27] Nano drug delivery systems provide an effective way to overcome this obstacle as they are able to cross the BBB through specific design and modifications.[28] Therefore, delivery of natural drug molecules using nanocarriers can improve drug solubility, bioavailability, and BBB penetration, leading to the development of effective and safe drugs for stroke therapy. For example, xiao et al developed a novel nitric oxide-driven nanomotor for synergistic treatment of ischemic stroke by loading tanshinone IIA with mesoporous dopamine nanomaterials and mediating the transport of nanoparticles (NPs) to the stroke region by modifying the stroke homing peptide on the nanoparticle surface.[29] Tang et al fused 4T1 tumor cell membranes with platelet membranes and further covered them on the surface of liposomes loaded with paeonol and polymetformin to obtain a biomimetic

nanoplatform for ischemic stroke therapy.[30] Liu et al developed a populin oligomer nanoparticle, a strategy to penetrate the BBB through multiple receptor-mediated transcytosis, remodel the BBB through protective autophagy, and modulate the post-stroke microenvironment.[31]

In this study, a brain tissue-targeted Cur@GAR NPs was developed as an ischemic stroke therapeutic agent. The NPs mainly comprised Cur, gelatin and the RVG29. As shown in Scheme 1, Cur@Gel NPs was first prepared by pH cycling. Then, RVG29 and aldoxylated hyaluronic acid (AHA) were mixed with Cur@Gel NPs. RVG29 was modified on the surface of Cur@Gel NPs through the Schiff base of AHA with gelatin and the addition reaction of the aldehyde group with the thiol group in RVG29. Previous studies have demonstrated that RVG29 is a neuron-targeting peptide that can bind to the nicotinic acetylcholine receptor (nAchR) on the surface of neuronal cells, thereby enhancing the cellular internalization of NPs and mediating the efficient passage of NPs across the BBB, possibly through nAchR-mediated transcytosis and receptor-mediated endocytosis.[32,33] The results showed that Cur@GAR NPs possess good dispersion and stability, which is favorable for injection drug delivery. In cells exposed to H_2O_2, Cur@GAR NPs exhibited remarkable ROS scavenging capability and cytoprotective effects, resulting in substantial reduction in cell death. Additionally, the cellular uptake of Cur@GAR NPs was significantly enhanced compared to Cur@Gel NPs. In a rat stroke model, treatment with Cur@GAR NPs reversed neurobehavioral deficits and ameliorated neuroinflammation in brain tissue. Further, both in vivo and in vitro studies demonstrated that Cur@GAR NPs are biocompatible with no significant side effects. In light of these observations, Cur@GAR NPs offer a novel strategy for developing stroke therapies with targeted, multipotent effects and low side effects.

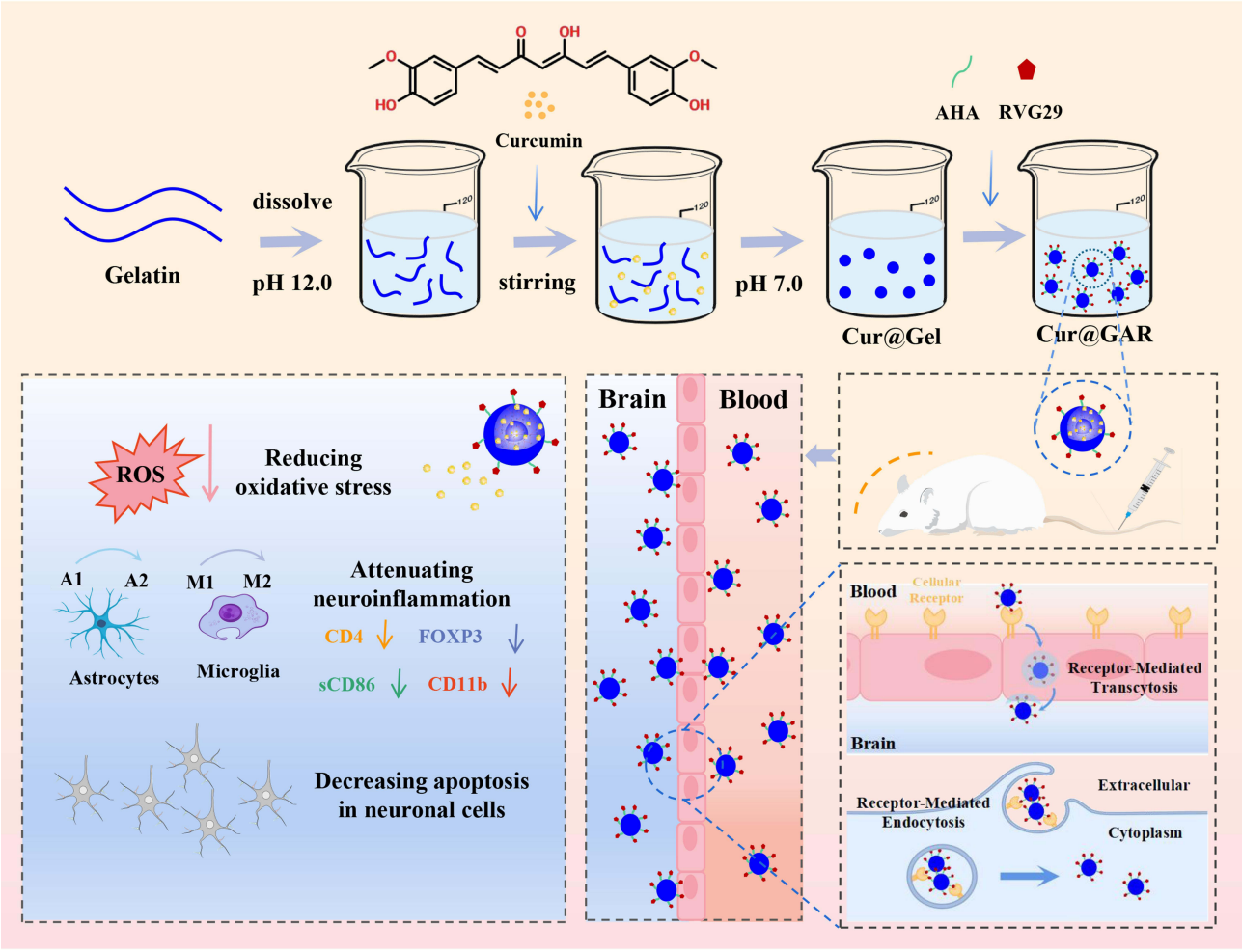

Scheme 1 Construction of Cur@GAR NPs and its role in stroke treatment.

Experimental and Methods

Materials

Bovine bone gelatin and hyaluronic acid were provided by Shanghai Macklin Biochemical Co., Ltd (Shanghai, China). Curcumin was supplied by Shanghai Aladdin Bio-Chem Technology Co., Ltd (Shanghai, China). DPPH radical scavenging assay kit and Elisa-kit was purchased from Shanghai Keaibo Biotechnology Co., Ltd (Shanghai, China).

Synthesis of Cur@GAR NPs

Cur@Gel NPs were prepared through pH cycling method. Briefly, 1.0 g of gelatin was soaked in 100 mL of ultrapure water for 10 min, prior to being dissolved at 45 °C with stirring. Subsequently, the solution's pH was raised to 12.0 using 4 mol/L NaOH. After 5 minutes of magnetic stirring, 0.1 g of Cur was added, and stirring continued for 30 min. Afterwards, the pH of the mixture was adjusted to 7.0 using 1 mol/L HCl and centrifuged at 1375 ×g. The resulting supernatant was freeze-dried to obtain Cur@Gel.

The preparation of AHA was started with weighing 2.0 g of hyaluronic acid and dissolving it in 200 mL of Phosphate buffers (pH 5.0). Then, 1.0 g of sodium periodate was added, and the resulting mixture underwent a 5-hour reaction in the dark. After terminating the reaction with ethylene glycol (2 mL), the solution was dialyzed for 5 days and lyophilized to obtain AHA.

To modify the brain-targeting ligand RVG29 peptide to the Cur@Gel surface, RVG29 (10 mg) and AHA (5 mg) were added into 25 mL of Cur@Gel dispersion (pH 8.5). After 24 h of reaction in the dark, the Cur@GAR NPs were collected by centrifugation and freeze-dried.

Characterization of Nanoparticles

The synthesis of AHA was verified by 1H NMR and FTIR. The particle size and morphological structure of Cur@Gel NPs and Cur@GAR NPs were analyzed using transmission electron microscopy (TEM). The distribution and content of elements in Cur@GAR NPs were determined using Energy Dispersive X-ray Spectroscopy (EDS).

To study the release behavior of curcumin, Cur@GAR NPs (1 mg/mL) was added to PBS and incubated at 37 °C. At different time intervals, 2 mL of Cur@GAR NPs dispersion was taken, centrifuged and the absorbance of the supernatant was measured at 425 nm.

In addition, Cur@GAR NPs (100 μg/mL) were dispersed in deionized water, PBS and DMEM to observe their stability and dispersion. On day 9, the degradation of Cur@GAR NPs was observed by SEM.

In vitro Antimicrobial Properties Evaluation

To assess the antibacterial properties of the resulting nanoparticles, antibacterial assays were conducted using Staphylococcus aureus (*S. aureus*) and Escherichia coli (*E. coli*). 100 μL of Gel, Cur@Gel NPs and Cur@GAR NPs (1 mg/mL) were mixed with 900 μL of bacterial suspension (1×10^6 CFU/mL), respectively. After 2, 4 and 8 hours of co-culture, the bacterial suspension was diluted and spread on LB agar medium. The colonies were photographed and counted after incubation in an incubator at 37 °C for 24 h. The experiment was repeated three times in parallel.

Antioxidant Properties Evaluation

The antioxidant activity of the resulting nanoparticles was investigated using DPPH radical scavenging assay kit. The nanoparticles (1 mg/mL) were mixed with nitrogen radical extract in the ratio of 1:9 by shaking, and the supernatant was taken for the assay after centrifugation. Sample supernatant (0.2 mL), anhydrous ethanol (0.9 mL) and DPPH reagent (0.9 mL) was mixed in the centrifuge tube, and a blank tube, a positive control tube and a sample control tube were set up at the same time. After mixing, the reaction was run for thirty minutes at ambient temperature and without illumination. The UV-visible scanning spectra at 400–800 nm were detected, and the change of absorbance of the samples at 517 nm was observed.

Biocompatibility Evaluation

Human neuroblastoma cells (SH-SY5Y, purchased from Wuhan Shangen Biotechnology Co., Ltd) were used to evaluate the biocompatibility of Cur@GAR NPs. The effects of various NPs concentrations (10, 25, 50, and 100 μg/mL) on cell viability were examined by CCK-8 assays. Briefly, 100 μL of SH-SY5Y cells (104 cells/mL) was inoculated into 96-well plates. The medium containing different concentrations of nanoparticles was replaced after 24 h of incubation. After 48 h of treatment, CCK-8 reagent was added to co-incubate for 1 h and the absorbance of cells at 450 nm was detected. Subsequently, SH-SY5Y cells were exposed to Cur@GAR NPs (100 μg/mL). The live-dead cell staining experiment was used to evaluate the cytotoxicity of the nanoparticles following a 48-hour incubation period. Additionally, the number and morphology of SH-SY5Y cells were observed by crystal violet staining.

Fresh mouse blood was employed to assess the hemocompatibility of the Cur@GAR NPs. 30 μL of mouse erythrocytes were co-incubated with 1 mL of saline containing Cur@GAR NPs, and shaking at 37 °C for 1 h. After incubation, the absorbance at 540 nm was measured after centrifuging the supernatant. The following formula was used to determine the nanoparticles' hemolysis ratio:

$$\text{Hemolysis ratio}(\%) = \frac{\text{Abs}_{\text{sample}} - \text{Abs}_{\text{negastive}}}{\text{Abs}_{\text{positive}} - \text{Abs}_{\text{negative}}} \times 100\%$$

Intracellular ROS Protection of Nanoparticles

To assess the intracellular ROS scavenging and cytoprotective ability of Cur@GAR NPs, H_2O_2 solution (200 μM) was utilized to induce intracellular ROS. SH-SY5Y cells were inoculated into 6-well plates and cultured until the cell fusion was about 90%. Then the cells were subjected to a 2-hour H_2O_2 treatment. After washing with PBS, a medium containing 100 μg/mL Cur@Gel NPs or Cur@GAR NPs was added. After treatment for 6 h, 10 μM 2′, 7′-dichlorofluorescein diacetate (DCFH-DA) was used to stain the cells. Inverted fluorescence microscopy was used to observed intracellular ROS. In addition, the survival status of ROS-rich cells after nanoparticle treatment was assessed by live-dead cell staining and Hoechst 33342 staining.

Cellular Uptake of Nanoparticles

To study the internalization of Cur@GAR NPs by neuronal cells, the nanoparticles were labeled using rhodamine B (RhB) and cellular uptake experiments were performed in SH-SY5Y cells. Initially, RhB (containing carboxyl groups) was dissolved in MES buffer. EDC and NHS were added and stirred overnight to activate the carboxyl groups. Subsequently, Cur@Gel NPs or Cur@GAR NPs (containing amine groups) were introduced separately and stirred continuously for 24 hours. The resulting mixture was then dialyzed in pure water for 5 days to remove unreacted EDC/NHS and RhB. Post-dialysis, the product was lyophilized to yield RhB-labeled NPs (Cur@Gel-RhB and Cur@GAR-RhB). Prior to use, these NPs were resuspended in DMEM medium (100 μg/mL) and their fluorescence was visualized and quantified under a fluorescence microscope.

SH-SY5Y cells were cultured in 6-well plates (4×10^5 cells/well) and treated with DMEM medium containing Cur@Gel, Cur@GAR, Cur@Gel-RB NPs or Cur@GAR-RB NPs. After 6 hours of co-incubation, cells were washed 3 times using PBS to remove uninternalized nanoparticles. Subsequently, cells were fixed with 4% paraformaldehyde and permeabilized with 0.1% Triton X-100 at room temperature. After staining the nuclei with DAPI, the cells were visualized by inverted fluorescence microscopy.

Construction of Rat Ischemic Stroke Disease Model

MCAO is a widely recognized model of cerebral ischemia on an international scale, with a pathophysiological mechanism that closely resembles that of human ischemic stroke. Moreover, owing to the similarity of rat cerebral vascular anatomy and neurons to those of higher mammals, along with their high reproducibility and cost-effectiveness, rats have increasingly been employed in recent years to develop models of cerebral ischemia. Therefore, the in vivo efficacy of Cur@GAR NPs on ischemic stroke was investigated using the MCAO rat model.[34,35] All animals were handled strictly in accordance with the animal ethical procedures and guidelines of the People's Republic of China, and this study was approved by the Animal Ethics Committee of the Eighth Affiliated Hospital of Sun Yat-sen University. The rats were anesthetized intraperitoneally

before undergoing surgery for modeling stroke disease. First, the rat's head was fixed with incisors, followed by isolating the muscle fascia of neck with surgical tools, severing the distal external carotid artery, and clamping the common carotid artery with vascular clips. A fish line with a rounded tip was placed about 2 cm into the external carotid artery after a little incision was made in the wall. Subsequently, the vascular clamp of the common carotid artery was opened, and the myofascial skin of the rats was sterilized and sutured. After 2 hours, the wire was withdrawn about 2 cm and the rats were observed. If the rat exhibits hemiplegia on one side of its body and rotates predominantly in one direction upon lifting its tail, the modeling is deemed successful. In the animal experiments, the experimental rats were divided into four groups: Normal, Model, Cur@Gel, and Cur@GAR. Normal groups were sham-operated rats treated with saline, and the Model, Cur@Gel, and Cur@GAR groups were stroke rats treated with saline, Cur@Gel NPs (20 mg/kg), and Cur@GAR NPs (20 mg/kg), respectively (administered by intravenous injection once daily for 7 days).

Morris Water Maze Experiment

On days 1, 4, and 7 of administration, the Morris water maze experiment and the open field experiment were used to conduct behavioral tests on experimental rats. For the Morris water maze task, an underwater platform and spatial markers were set up in a 160 cm diameter pool. The pool was filled with water to a level that could just submerge the platform by 1–2 cm. In the learning phase, rats were allowed to observe at the underwater platform for around 30 seconds. The rats were positioned in the water maze from various spatial markers throughout the test phase, and their behaviors were observed for 2 min. A digital camera tracked the rats' paths and the amount of time they spent climbing to the underwater platform.

Open Field Experiment

Open field experiments were conducted in a square reaction box of size 80 cm*80 cm*50 cm. After the rats were placed in this box, their behaviors were recorded for 3 min using a digital camera, including the number of squares, exercise duration and the number of uprights of the rats.

In vivo Stroke Treatment

On days 7 of administration, the experimental rats were euthanized in accordance with ethical regulations and their brain tissues were removed, rinsed with saline, and fixed. The fixed brain tissue was then dehydrated and processed for paraffin embedding, and the cured tissue was cut into thin slices. Histological analysis was performed using H&E staining. Additionally, to assess the neuroinflammatory status, the expression of caspase-3 (CASP-3), ionized calcium binding adaptor molecule-1 (IBA-1), glial fibrillary acidic protein (GFAP), and myeloperoxidase (MPO) was detected by immunofluorescence staining. CSAP-3, cluster of differentiation 4 (CD4), recombinant integrin alpha M (CD11b), forkhead box protein 3 (FOXP3), soluble cluster of differentiation 86 (sCD86), and recombinant mannose receptor C type 1 (MRC1) were detected by the Elisa-kit.

In vivo Toxicity Assessment

To study the in vivo toxicity of Cur@GAR NPs, heart, kidney, liver, spleen, and lung were collected from experimental rats at the end of the experiment and analyzed histologically by H&E staining.

Statistical Analysis

The mean ± SD was used to present the experimental data. Every experiment was run through at least three times, and the Student's *t*-test was used in the statistical analysis using the GraphPad Prism program. In the analysis, significance values of $*p < 0.05$, $**p < 0.01$, and $***p < 0.001$ were applied.

Results and Discussions

Fabrication and Characterization of Cur@GAR NPs

To prepare Cur@GAR NPs targeting brain tissues, Cur@Gel NPs were first prepared by encapsulating Cur into bovine bone gelatin using the pH cycling method. Subsequently, the RVG29 peptide was modified to the surface of

Cur@Gel NPs to form Cur@GAR NPs (Figure 1C). The synthesis of AHA was confirmed through FTIR and ^{1}H NMR analyses. In the ^{1}H NMR spectrum, the peaks at 4.9 ppm, 5.0 ppm, and 5.1 ppm corresponded to the hemiacetal proton and neighboring hydroxyl group, respectively (Figure 1A).[36,37] In the FTIR spectrum, the stretching vibrations of the carbonyl (C=O) and the methyl (CH) groups in the aldehyde (-CHO) were observed at 1730 cm^{-1} and 2939 cm^{-1}, respectively (Figure 1B). These findings signify the successful production of AHA. Additionally, the formation and surface morphology of Cur@Gel NPs and Cur@GAR NPs were observed by TEM. As shown in Figure 1D, the Cur@Gel NPs exhibited irregularly spherical shapes, and the Cur@GAR NPs displayed a regular spherical morphology. Particle size analysis showed that the Cur@Gel NPs had an average particle size of 90.54 ±11.66 nm. After surface modification with the RVG29 peptide, there was a slight increase in the size of the Cur@GAR NPs, with an average particle size of 141.27±32.93 nm (Figure 1E). In addition, the Energy Dispersive Spectrometry (EDS) analysis revealed the existence of C (red), N (yellow), O (green), and S (purple) elements in the Cur@GAR NPs (Figure 1F and G). The presence of S elements indicated that the RVG29 was successfully encapsulated onto the surface of the Cur@Gel NPs. Together these results demonstrated the successfully fabrication of Cur@GAR NPs.

Next, the release behavior of Cur in Cur@GAR NPs was examined. As shown in Figure 1H, Cur was gradually released in PBS over time. At 48 h, the cumulative release of Cur reached 61.57±4.0%, which facilitated the inhibition of neuroinflammation and scavenging of ROS quickly, and thus assisting in promoting vascular production and tissue repair. The dispersion and stability of Cur@GAR NPs were subsequently evaluated, with 100 μg/mL of Cur@GAR NPs and Cur being dispersed in PBS and stored at room temperature. Results showed that Cur@GAR NPs had good dispersion and stability. Specifically, after preservation for 8 h, the Cur@GAR NPs suspension was clear and transparent with no visible precipitation sedimentation or turbidity. Whereas, obvious precipitation of Cur could be observed in the curcumin solution (Figure 1I). It could thus be seen that the encapsulation of Cur into gelatin nanoparticles could significantly improve its solubility. Besides, the stability of Cur@GAR NPs in deionized water, PBS and DMEM was observed, with results indicating that Cur@GAR NPs were well dispersed and stable in different solutions (Figure 1I). On the 9th day of storage, turbidity and precipitation in the Cur@GAR NPs solution could be visible to the unaided eye, and the degradation of Cur@GAR NPs was observed by SEM. These observations suggested the good dispersion and stability of Cur@GAR NPs, which could be conducive to maintaining their efficacy and safety during in vitro injectable drug delivery.

Antimicrobial and Antioxidant Effects of Cur@GAR NPs

The antimicrobial properties of Cur@GAR NPs were studied using the plate counting method. The results showed that *S. aureus* and *E. coli* treated with Cur@Gel NPs or Cur@GAR NPs formed significantly fewer colonies in LB agar plates (Figure 2A). After 8 hours of treatment, Cur@GAR NPs exhibited antibacterial ratio of 93 ± 2.83% and 75.5 ± 3.54% against *S. aureus* and *E. coli*, respectively (Figure 2B and C). The good antimicrobial capacity of Cur@GAR NPs allows them to effectively prevent and manage possible infections during treatment, avoiding bacterial infections that could aggravate the condition and hinder recovery.

One of the key factors triggering ischemia/reperfusion injury is oxidative stress. Overproduction of radicals can occur during ischemia and reperfusion at the beginning of a stroke.[38] These free radicals are highly reactive and exacerbate the pathological process of stroke by damaging cell membranes, DNA and proteins, accelerating cell death and tissue damage.[39,40] Therefore, alleviation of oxidative stress is essential for the prevention and treatment of neurological damage after stroke. Cur@GAR NPs' antioxidant potential was evaluated using DPPH tests. As shown in Figure 2D, the DPPH radical alcohol solution in the blank group was purple in color, and the addition of Cur@Gel NPs and Cur@GAR NPs resulted in a significant discoloration of the solution. In UV-visible spectra, the absorbance of DPPH alcohol solution at 517 nm was significantly reduced in Cur@Gel and Cur@GAR groups. Quantitative analysis showed that the DPPH scavenging ratio was 58.67±0.58% and 65.67±1.53% for Cur@Gel NPs and Cur@GAR NPs, respectively (Figure 2E). Collectively, these results indicate that Cur@GAR NPs could help alleviate oxidative stress via scavenging free radicals.

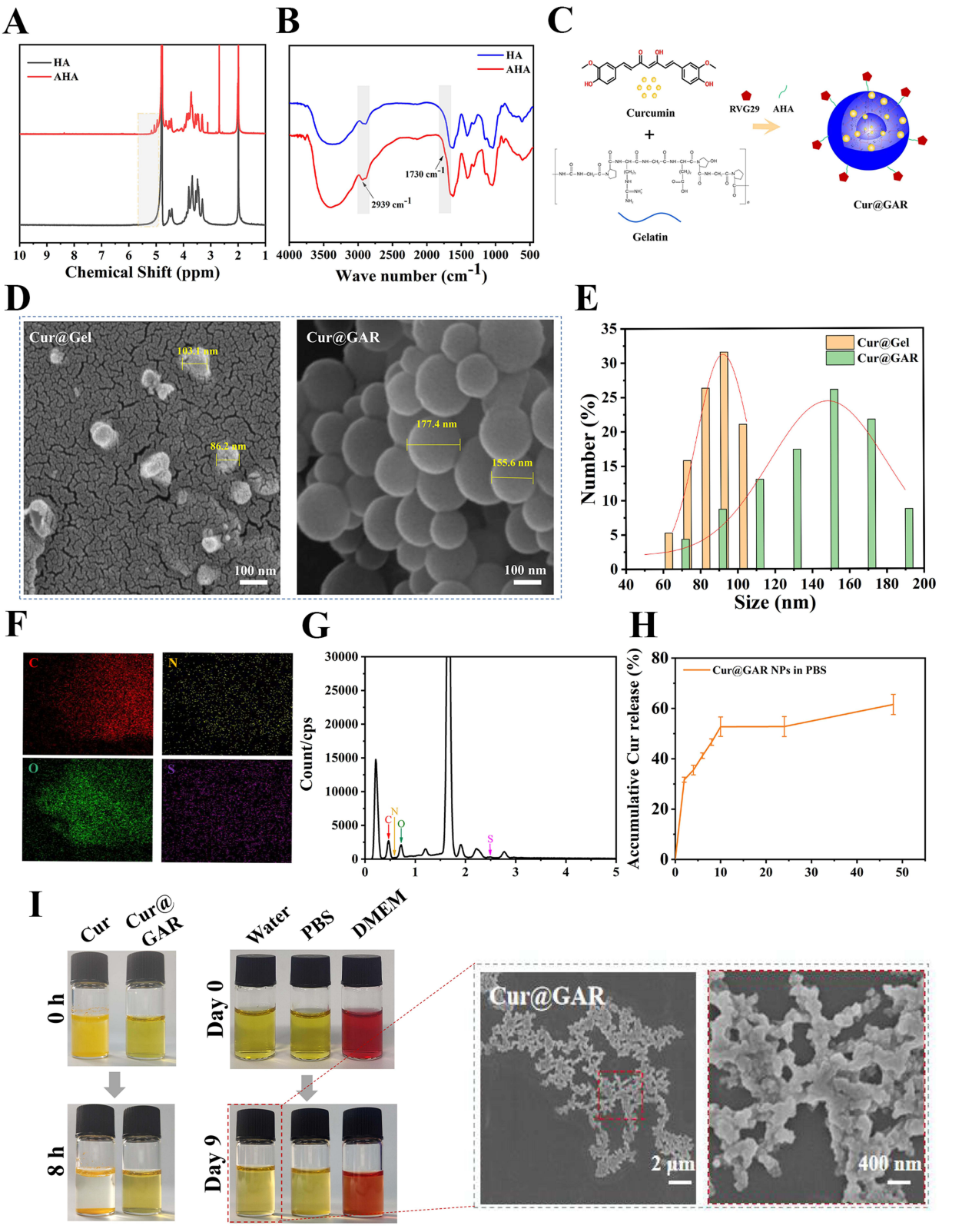

Figure 1 (**A**) ^{1}H NMR and (**B**) FTIR spectrum of HA and AHA. (**C**) Synthesis of Cur@GAR. (**D**) SEM images and (**E**) particle size distribution of Cur@Gel NPs and Cur@GAR NPs. (**F**) EDS mapping and (**G**) spectrogram of the total number of distribution maps of Cur@GAR NPs. (**H**) Curcumin release from Cur@GAR NPs in PBS. (**I**) Observation of the stability of Cur@GAR NPs.

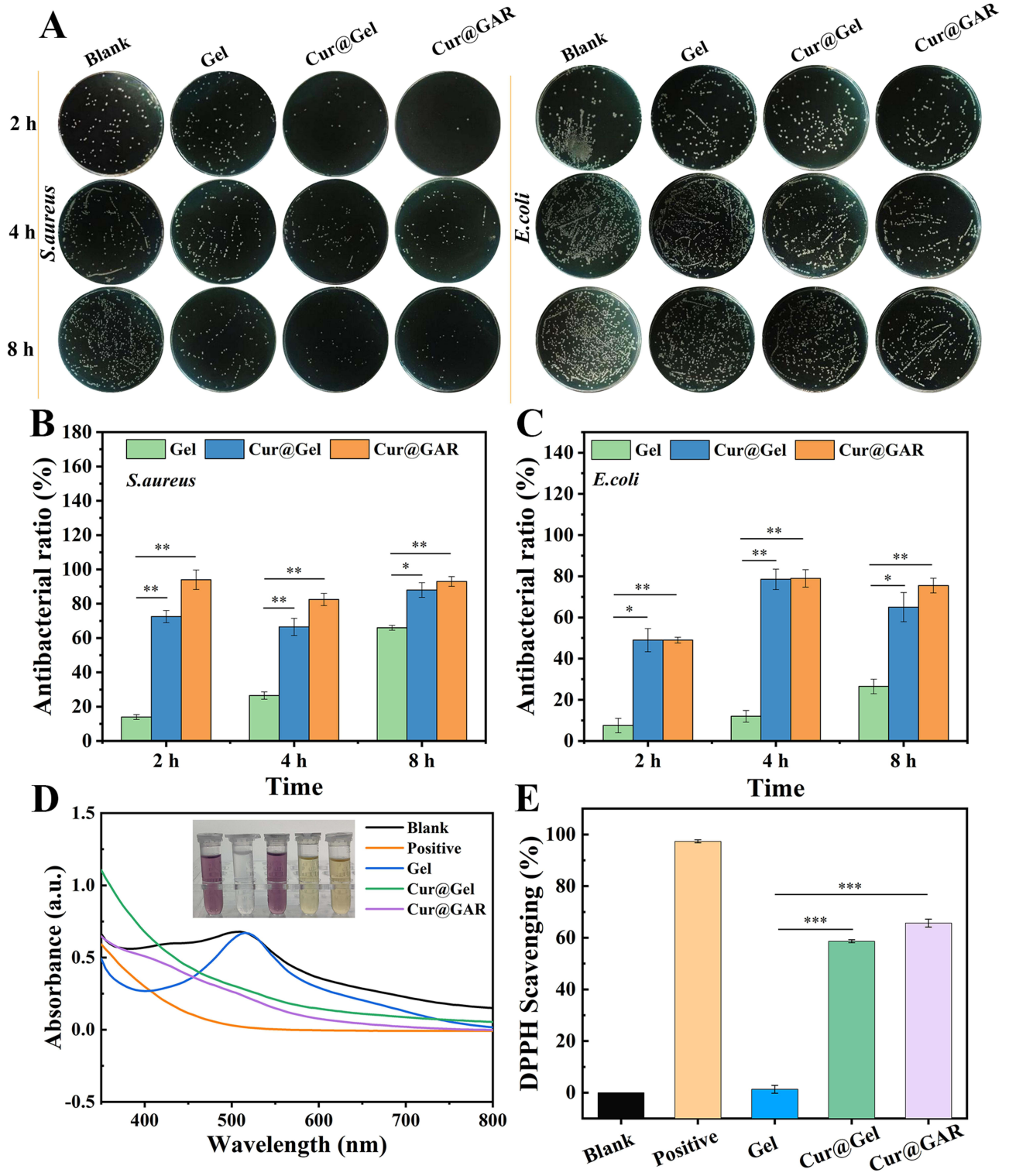

Figure 2 (**A**) Photographs of bacterial colonies of Gel, Cur@Gel NPs, and Cur@GAR NPs treatments. (**B**) Antibacterial ratio of S. aureus and (**C**) E.coli. (**D**) UV-visible spectrogram of the DPPH assay. (**E**) DPPH scavenging ratio of Gel, Cur@Gel NPs, and Cur@GAR NPs. Significance levels of *p< 0.05, **p< 0.01, and ***p<0.001 were applied.

Biocompatibility, Cellular Internalization, and Intracellular ROS Protection of Cur@GAR NPs

Good biocompatibility is thought to be a prerequisite for nanoparticles' application for in vivo therapy. To investigate the cytocompatibility of Cur@GAR NPs, the effects of Cur@Gel NPs and Cur@GAR NPs on the viability of SH-SY5Y cells were examined using CCK-8 assays. The results showed that Cur@Gel NPs and Cur@GAR NPs did not exhibit cytotoxicity even when treated at a high concentration (100 μg/mL) for 48 h (Figure 3A). Furthermore, the viability and morphology of SH-SY5Y cells were assessed by live-dead cell staining and crystal violet staining 48 hours after being treated with Cur@Gel NPs or Cur@GAR NPs (Figure 3B). Live-dead cell staining images showed that the SH-SY5Y cells survived well after Cur@Gel NPs or Cur@GAR NPs treatment and did not show increased dead cells. Crystal violet staining images showed that the cells in the Cur@Gel and Cur@GAR groups had normal cell morphology with clear outlines and good spreading. Taken together, these findings indicate that the resulting Cur@GAR NPs have good cytocompatibility.

To investigate the internalization of Cur@GAR NPs by neuronal cells, a cellular uptake experiment was conducted using SH-SY5Y cells. The results indicated that after co-incubating SH-SY5Y cells with Cur@Gel-RhB NPs or Cur@GAR-RhB NPs for 6 hours, a significantly greater red fluorescence was observed in the Cur@GAR-RhB group (Figure 3C). This finding suggests that RVG29 aids in the uptake of Cur@GAR NPs by neuronal cells and enhances the transport of Cur@GAR NPs across the BBB.

Next, the protective effect of Cur@GAR NPs against oxidative stress-induced cell death was investigated. Substantial levels of ROS were initially generated in SH-SY5Y cells by exposure to H_2O_2. Then, intracellular ROS content was detected using a DCFH-DA fluorescent probe, while normal cells were labeled using Hoechst 33342, and cell activity was detected through a live-dead cell staining assay. As shown in Figure 3D, the ROS content in H_2O_2-treated cells was significantly increased, while Hoechst staining showed decrease number of blue-fluorescent normal cells, and live-dead cell staining revealed a significant reduction in cell survival, with a large number of red dead cells. In contrast, in cells co-treated with H_2O_2 and NPs (Cur@Gel NPs or Cur@GAR NPs), intracellular ROS production was significantly reduced and no significant decrease in cell survival was observed. These results suggest that Cur@GAR NPs were able to scavenge intracellular ROS in a timely and effective manner and reduce H_2O_2-induced cell death and injury. This phenomenon may be attributed to the potent antioxidant capacity of Cur. Therefore, Cur@GAR NPs could assist in safeguarding brain tissue, minimizing neurological impairment following a stroke, and promoting neurological recovery.

In addition, the blood compatibility of Cur@GAR NPs was investigated by hemolysis test. The results showed that Cur@GAR NPs had good compatibility with mouse erythrocytes. The hemolysis ratio was just 0.59 ± 0.057% when the content of Cur@GAR NPs was 100 μg/mL, which was significantly lower than the allowed threshold (5%) (Figure 3E). Besides, the erythrocyte supernatants treated with different concentrations of Cur@GAR NPs revealed a light yellow similar to the negative control (Figure 3F). These results collectively illustrate the high biocompatibility and neuroprotective efficacy of Cur@GAR NPs, supporting further investigation into their therapeutic capabilities in vivo.

Cur@GAR NPs Improve Behavioral Deficits After Stroke

Given the BBB penetration ability, potent antioxidant properties and high biocompatibility of Cur@GAR NPs in in vitro experiments, a rat stroke disease model was used to further validate their effectiveness in vivo. The rat model of ischemic stroke was constructed by carotid artery ligation, and successful rats showed hemiparesis of one side of the limb and rotation only along one side after the tail was lifted. The experimental rats were split up into four groups: Cur@Gel, Cur@GAR, Model, and Normal. On days 1, 4 and 7 after surgery, the open field experiment and the Morris water maze experiment were used for behavioral assessment in rats. Figure 4A shows a schematic diagram of the response box for the open-field test and the trajectory of the experimental rat over 180 s (blue indicates the starting point and green indicates the end point). It could be observed that rats in the Model group displayed fewer movement trajectories in the reaction box than normal rats. Correspondingly, quantitative analyses revealed that the Model group exhibited a notable decrease in the number of squares and exercise duration. In contrast, the rats' trajectory in Cur@Gel and Cur@GAR groups significantly increased in comparison to the Model group (Figure 4C and D). Besides, the number of uprights is

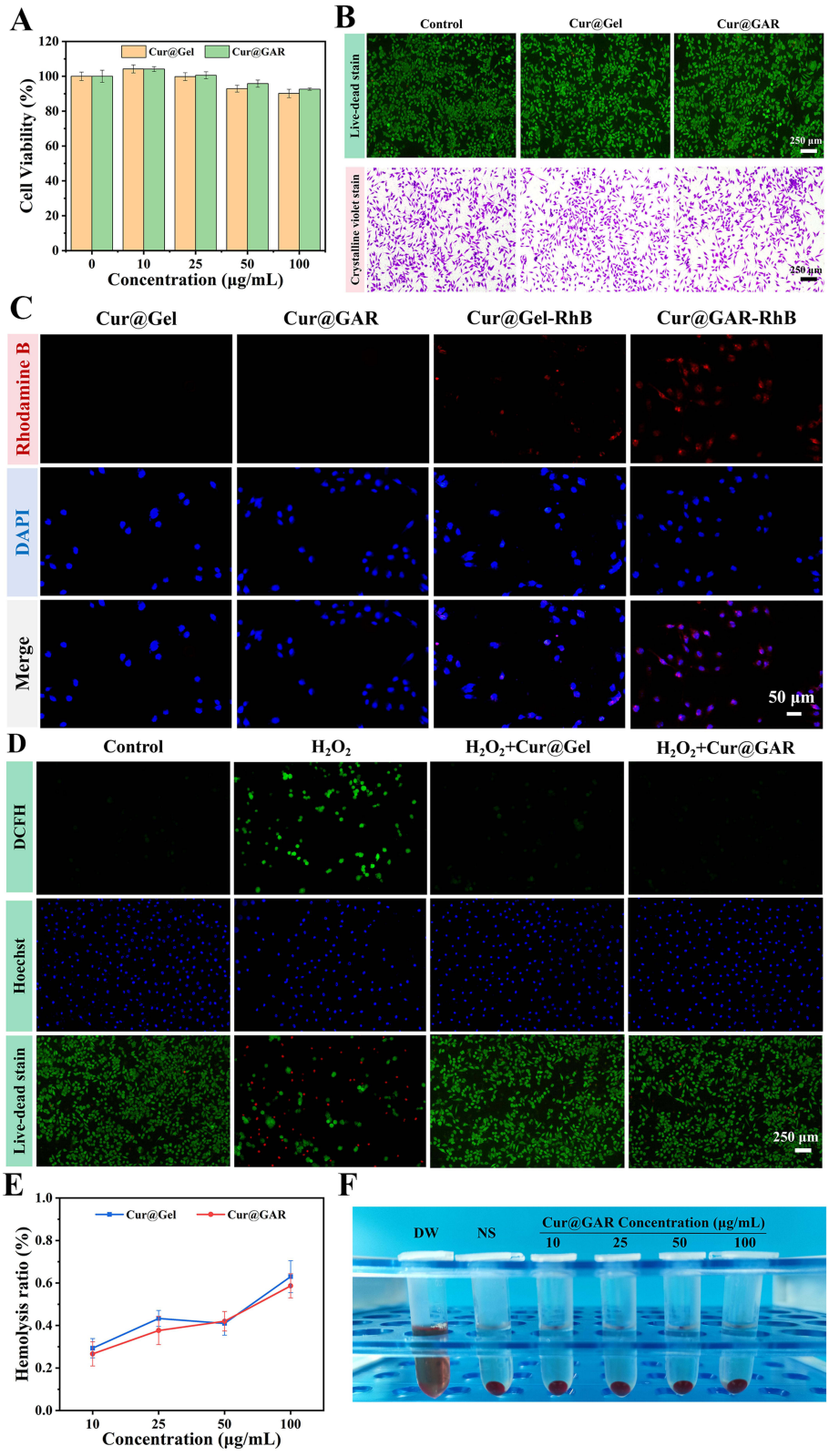

Figure 3 (**A**) Viability of SH-SY5Y cells treated with varying amounts of Cur@Gel NPs and Cur@GAR NPs in CCK-8 assay. (**B**) Pictures of live-dead cell staining and crystal violet staining of SH-SY5Y cells treated with Cur@Gel NPs and Cur@GAR NPs. (**C**) Internalization of Cur@Gel-RhB NPs and Cur@GAR-RhB NPs in SH-SY5Y cells. (**D**) Effects of Cur@Gel NPs and Cur@GAR NPs on intracellular ROS content and cytotoxicity in H_2O_2-treated SH-SY5Y cells. (**E**) Hemolysis ratio of Cur@Gel NPs and Cur@GAR NPs. (**F**) Pictures of erythrocytes treated with different concentrations of Cur@GAR NPs.

https://doi.org/10.2147/IJN.S487628 DovePress

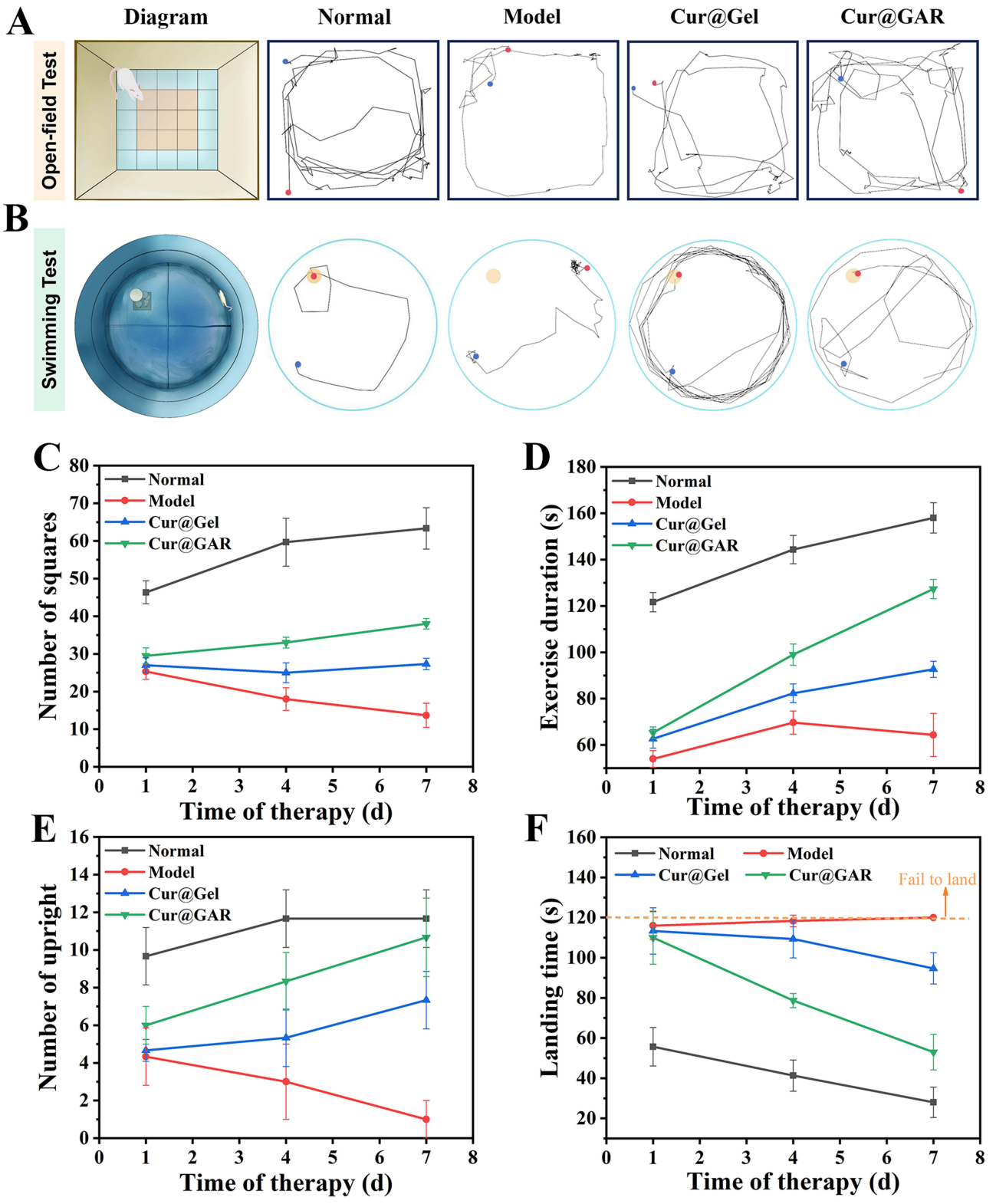

Figure 4 (**A**) Schematic diagram and movement trajectories of experimental rats of the open field test and (**B**) the swimming test. (**C**) Number of squares, (**D**) exercise duration and (**E**) number of uprights of experimental rats in the open field experiment. (**F**) Landing time of experimental rats in the swimming test.

one of the indicators to assess the exploratory behavior and activity level of rats. During the experiment, the stroke rats showed a lower number of uprights, whereas rats in the Cur@Gel and Cur@GAR groups demonstrated a significantly higher number of uprights than the Model group (Figure 4E). These results suggest that ischemic stroke significantly

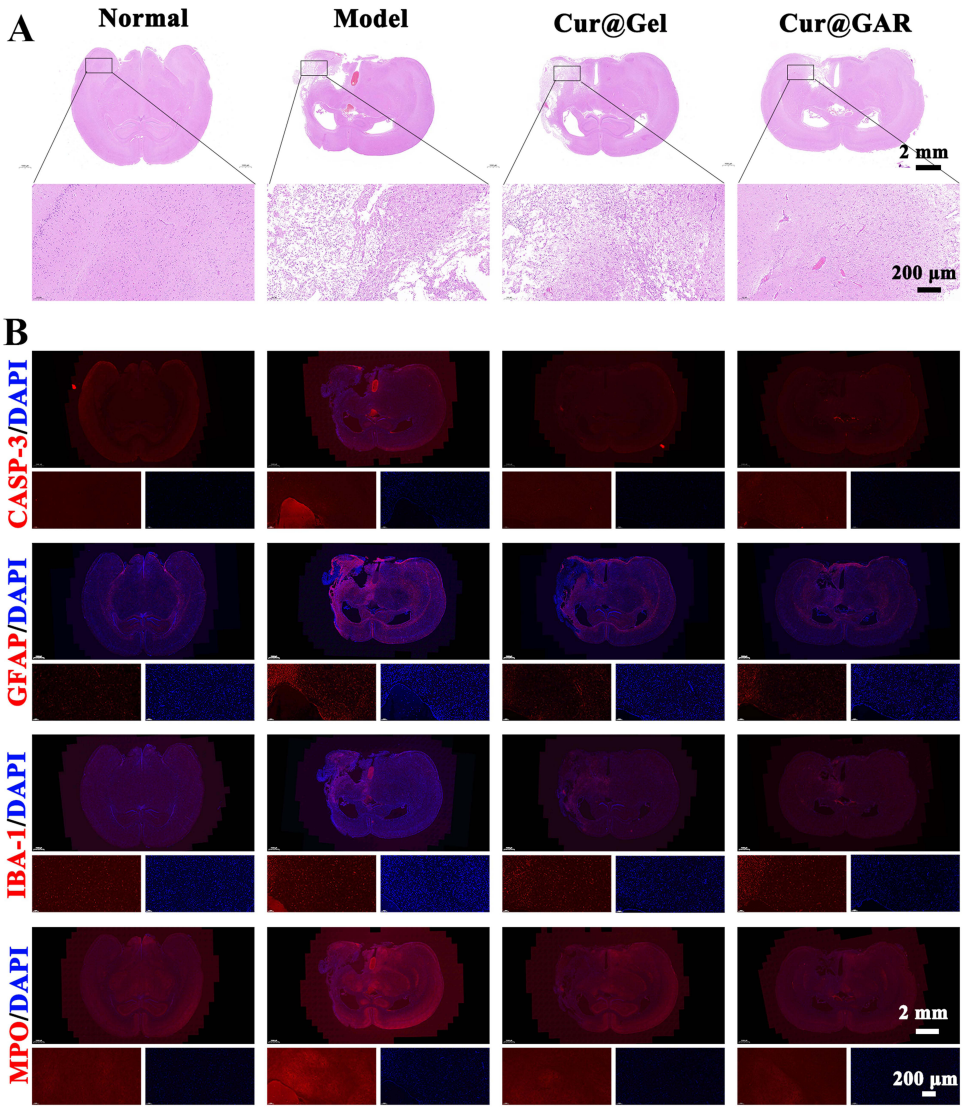

Figure 5 (**A**) H&E staining images of brain tissue sections from experimental rats on day 7 after surgery. (**B**) Immunofluorescence staining images of CASP-3, GFAP, IBA-1, and MPO in brain tissue sections of experimental rats on day 7 after surgery.

reduced locomotion and activity levels in rats, and treatment with Cur@Gel and Cur@GAR NPs partially restored these functions. Notably, Cur@GAR NPs exhibited better therapeutic efficacy than Cur@Gel NPs, suggesting that the encapsulation of RVG29 significantly improved the efficacy of nanoparticles.

Figure 4B shows a schematic representation of the Morris water maze experiment and the experimental rats' movement trajectories over 120 s (blue indicates the starting point and green indicates the end point). The behavioral abilities of the experimental rats were assessed by their landing time. According to the results, the rats in the Normal group were able to land on the platform quickly with an average landing time of 28 ± 7.55 s, in comparison, the rats in the Model group failed to land within 120 s and exhibited a shorter trajectory (Figure 4B and F). The rats treated with Cur@GAR NPs showed a significantly shorter landing time, with an average landing time of 53±8.89 s, suggesting that treatment with Cur@GAR NPs significantly improved the behavioral abilities of the rats (Figure 4F). Moreover, Cur@GAR NPs demonstrated superior therapeutic efficacy to Cur@Gel NPs, with rats in the Cur@Gel group taking longer time to land and displaying longer locomotor trajectories. Taken together, the above results indicated the effectiveness of Cur@GAR NPs in ameliorating stroke-induced behavioral deficits, possibly due to Cur's neuroprotective

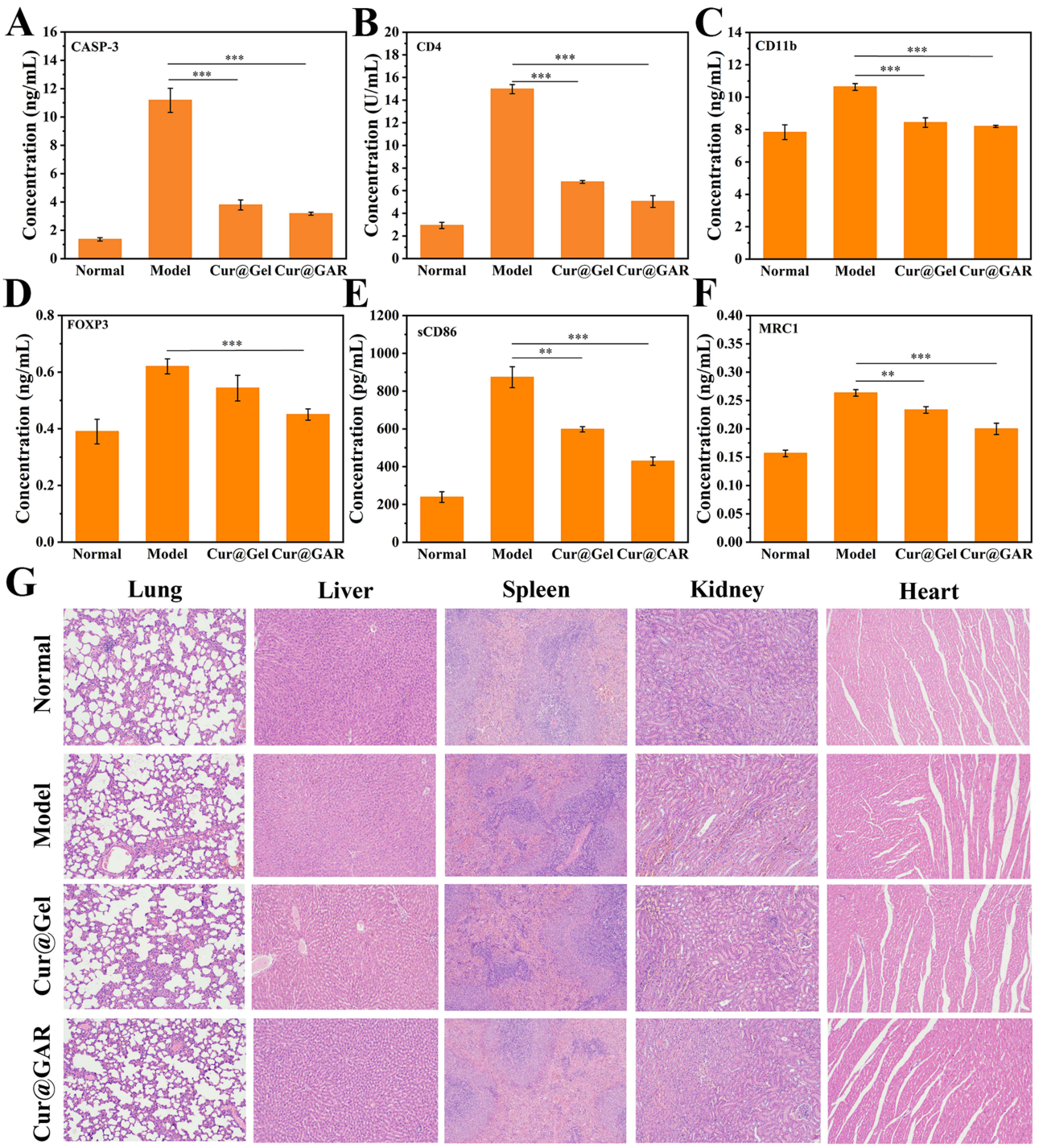

Figure 6 Elisa assay for (**A**) CASP-3, (**B**) CD4, (**C**) CD11b, (**D**) FOXP3, (**E**) sCD86 and (**F**) MRC1 in brain tissues of experimental rats at 7 days post-surgery. (**G**) H&E staining images of major organs of experimental rats at the end of the experiment. Significance levels of $^{**}p < 0.01$, and $^{***}p < 0.001$ were applied.

benefits from its anti-inflammatory and antioxidant qualities. The better efficacy of Cur@GAR NPs than Cur@Gel NPs may be due to the functionalization of the RVG29 peptide that promotes nanoparticle targeting to brain tissue and crossing the BBB.

In vivo Neuroprotective Effects of Cur@GAR NPs

To further verify the neuroprotective effects of Cur@GAR NPs, the brain tissues of experimental rats were pathologically analyzed. According to H&E staining, the brain tissues of normal rats were structurally intact with tightly arranged cells, whereas severe necrosis was observed in the Model group. Following the administration of Cur@GAR NPs, a notable decrease in the necrotic area of brain tissues was observed, indicating the protective effect of Cur@GAR NPs on brain tissue after stroke (Figure 5A).

Next, to investigate whether Cur@GAR NPs could reduce stroke-induced apoptosis, immunofluorescence labeling was utilized to identify the expression of CASP-3. The CASP-3 expression level in the Cur@GAR group was considerably lower than in the Model group, indicating that Cur@GAR was beneficial in reducing stroke-induced neuronal apoptosis (Figure 5B). In addition, strokes can trigger a strong inflammatory response in the brain. Following cerebral ischemia, the inflammatory cascade response is activated and mediated by a variety of molecules, leading to the generation of pro-inflammatory cytokines as well as ROS that exacerbate irreversible neuronal damage.[2] Astrocytes are the most numerous glial cells in the brain and undergo reactive proliferation during nerve injury or inflammation to participate in the inflammatory response.[41,42] Immunofluorescence staining results of GFAP showed that treatment with Cur@GAR NPs reduced astrocyte inflammation. Additionally, microglia are also activated, following cerebral ischemia, exemplified by undergoing morphological changes and secrete cytokines.[42,43] Immunofluorescence staining of IBA-1 demonstrated that Cur@GAR NPs treatment reduced microglia inflammation. Furthermore, immunofluorescence staining results of MPO indicated reduced neutrophil activation and infiltration in the Cur@GAR group, suggesting a reduced inflammatory response (Figure 5B). Besides, the Elisa assay revealed a notable elevation in the expression levels of CASP-3, CD4, CD11b, FOXP3, sCD86, and MRC1 in the rat model of stroke disease. Conversely, in the Cur@GAR group, the expression of these factors significantly decreased in comparison to the Model group, suggesting an attenuated inflammatory and immune response (Figure 6A–F). Collectively, these results suggested that Cur@GAR NPs can alleviate stroke-triggered inflammatory response, further assisting with reducing neuronal cell damage and apoptosis, protecting brain tissue, and restoring the nervous system.

At the end of the experiment, the major organs of experimental rats were analyzed histologically using H&E staining. The findings revealed no evident pathological toxicity or adverse effects in the lungs, liver, spleen, kidneys, and heart of the experimental rats, indicating that Cur@GAR NPs exhibit minimal toxicity in vivo, further supporting their in vivo application in treating of stroke (Figure 6G).

Conclusions

In summary, a curcumin-loaded gelatin nanoparticle (Cur@GAR) with brain tissue-targeting effect for treating ischemic stroke was successfully developed in this study. This nano drug delivery system significantly improves the solubility of Cur and has good biocompatibility. Notably, cellular uptake experiments showed that RVG29 enhanced the uptake of Cur@GAR NPs by neuronal cells. Additionally, Cur@GAR NPs protected cells from H_2O_2-induced oxidative stress and apoptosis, indicating their potential in reducing neuronal cell injury by mitigating oxidative stress. Furthermore, in vivo studies showcased the remarkable neuroprotective effects of Cur@GAR NPs by effectively reducing neuroinflammation and neuronal cell apoptosis. Treatment with Cur@GAR NPs significantly ameliorated behavioral dysfunction in the rat model of stroke. Therefore, based on findings of the current experiment, it seems reasonable to argue that Cur@GAR NPs could offer an appealing option to the efficient management of stroke. A further investigation into the mechanism of action of Cur@GAR NPs in ischemic stroke treatment, and validation of its therapeutic efficacy and safety in clinical trials will bring Cur@GAR NPs closer to clinical application.

Funding

This work was supported by the National Natural Science Foundation of China (grant number 82001356), the Shenzhen Science and Technology Program (grant number JCYJ20220818102016034), the Futian Healthcare Research Project (grant number FTWS2022015), the Guangdong Province General University Youth Innovative Talent Project (grant number 2019KQNCX062), and Guangdong Province University Characteristic Innovation Project (grant number 2020KTSCX063).

Disclosure

All authors have declared no conflicts of interest in this work. This paper is available on SSRN as a preprint https://papers.ssrn.com/sol3/papers.cfm?abstract_id=4894156.

References

1. Liu Z, Ran Y, Huang S, et al. Curcumin protects against ischemic stroke by titrating microglia/macrophage polarization. *Front Aging Neurosci*. 2017;9:233. doi:10.3389/fnagi.2017.00233
2. Tian X, Fan T, Zhao W, et al. Recent advances in the development of nanomedicines for the treatment of ischemic stroke. *Bioact Mater*. 2021;6(9):2854–2869. doi:10.1016/j.bioactmat.2021.01.023
3. Zhao Z, Wu C, He X, et al. miR-152-3p aggravates vascular endothelial cell dysfunction by targeting DEAD-box helicase 6 (DDX6) under hypoxia. *Bioengineered*. 2021;12(1):4899–4910. doi:10.1080/21655979.2021.1959864
4. Lohkamp KJ, Kiliaan AJ, Shenk J, et al. The impact of voluntary exercise on stroke recovery. *Front Neurosci*. 2021;15. doi:10.3389/fnins.2021.695138
5. Wang Q, Yang F, Duo K, et al. The role of necroptosis in cerebral ischemic stroke. *Mol Neurobiol*. 2023;61:3882–3898.
6. Chen W, Jiang L, Hu Y, et al. Nanomedicines, an emerging therapeutic regimen for treatment of ischemic cerebral stroke: a review. *J Control Release*. 2021;340:342–360. doi:10.1016/j.jconrel.2021.10.020
7. Liu L, Yang C, Lavayen BP, Tishko RJ, Larochelle J, Candelario-Jalil E. Targeted BRD4 protein degradation by dBET1 ameliorates acute ischemic brain injury and improves functional outcomes associated with reduced neuroinflammation and oxidative stress and preservation of blood–brain barrier integrity. *J Neuroinflammation*. 2022;19(1):168. doi:10.1186/s12974-022-02533-8
8. Wu F, Lai S, Fu D, et al. Neuroprotective effects and metabolomics study of protopanaxatriol (PPT) on cerebral ischemia/reperfusion injury in vitro and in vivo. *Int J Mol Sci*. 2023;24(2):1789. doi:10.3390/ijms24021789
9. Gu Y, Huang P, Cheng T, et al. A multiomics and network pharmacological study reveals the neuroprotective efficacy of Fu-Fang-Dan-Zhi tablets against glutamate-induced oxidative cell death. *Comput Biol Med*. 2022;148:105873. doi:10.1016/j.compbiomed.2022.105873
10. Bao Q, Hu P, Xu Y, et al. Simultaneous blood–brain barrier crossing and protection for stroke treatment based on edaravone-loaded ceria nanoparticles. *ACS Nano*. 2018;12(7):6794–6805. doi:10.1021/acsnano.8b01994
11. Zhi K, Raji B, Nookala AR, et al. PLGA nanoparticle-based formulations to cross the blood–brain barrier for drug delivery: from R&D to cGMP. *Pharmaceutics*. 2021;13(4):500. doi:10.3390/pharmaceutics13040500
12. Wu K-J, Wang Y-S, Hung T-W, et al. Herbal formula PM012 induces neuroprotection in stroke brain. *PLoS One*. 2023;18(2):e0281421. doi:10.1371/journal.pone.0281421
13. Yu L, Tao J, Zhao Q, Xu C, Zhang Q. Confirmation of potential neuroprotective effects of natural bioactive compounds from traditional medicinal herbs in cerebral ischemia treatment. *JIN*. 2020;19(2):373–384.
14. Zhu T, Wang L, Wang L-P, et al. Therapeutic targets of neuroprotection and neurorestoration in ischemic stroke: applications for natural compounds from medicinal herbs. *Biomed Pharmacother* 2022;148:112719. doi:10.1016/j.biopha.2022.112719
15. Gomez-Verjan JC, Zepeda-Arzate EA, Santiago-de-la-Cruz JA, et al. Unraveling the neuroprotective effect of natural bioactive compounds involved in the modulation of ischemic stroke by network pharmacology. *Pharmaceuticals*. 2023;16(10):1376. doi:10.3390/ph16101376
16. Ri MH, Xing Y, Zuo HX, et al. Regulatory mechanisms of natural compounds from traditional Chinese herbal medicines on the microglial response in ischemic stroke. *Phytomedicine*. 2023;116:154889.
17. Zhao W, Zeng M, Li K, et al. Solid lipid nanoparticle as an effective drug delivery system of a novel curcumin derivative: formulation, release in vitro and pharmacokinetics in vivo. *Pharm Biol*. 2022;60(1):2300–2307. doi:10.1080/13880209.2022.2136205
18. He T, Lin X, Su A, et al. Mitochondrial dysfunction-targeting therapeutics of natural products in Parkinson's disease. *Front Pharmacol*. 2023;14. doi:10.3389/fphar.2023.1117337
19. Chopra H, Bibi S, Singh I, et al. Nanomedicines in the management of Alzheimer's disease: current view and future prospects. *Front Aging Neurosci*. 2022;14:879114. doi:10.3389/fnagi.2022.879114
20. Rassu G, Sorrenti M, Catenacci L, et al. Conjugation, prodrug, and co-administration strategies in support of nanotechnologies to improve the therapeutic efficacy of phytochemicals in the central nervous system. *Pharmaceutics*. 2023;15(6):1578. doi:10.3390/pharmaceutics15061578
21. Huang M, Zhai BT, Fan Y, et al. Targeted drug delivery systems for curcumin in breast cancer therapy. *Int J Nanomed*. 2023;18:4275–4311.
22. Hussain Z, Thu HE, Ng S-F, et al. Nanoencapsulation, an efficient and promising approach to maximize wound healing efficacy of curcumin: a review of new trends and state-of-The-art. *Colloids Surf B*. 2017;150:223–241. doi:10.1016/j.colsurfb.2016.11.036
23. Chen Y, Lu Y, Lee RJ, Xiang G. Nano encapsulated curcumin: and its potential for biomedical applications. *Int J Nanomed*. 2020;15:3099–3120.
24. Jiang C, Zhou Y, Chen R, et al. Nanomaterial-based drug delivery systems for ischemic stroke. *Pharmaceutics*. 2023;15(12):2669. doi:10.3390/pharmaceutics15122669
25. Li C, Sun T, Jiang C, et al. Recent advances in nanomedicines for the treatment of ischemic stroke. *Acta Pharm Sin B*. 2021;11(7):1767–1788. doi:10.1016/j.apsb.2020.11.019
26. Zhong D, Gan Z, Zheng M, et al. Knowledge mapping of nano drug delivery systems across blood-brain barrier from 1996 to 2022: a bibliometric analysis. *Heliyon*. 2023;9(5):e15828. doi:10.1016/j.heliyon.2023.e15828
27. Song W, Bai L, Yang Y, et al. Long-circulation and brain targeted isoliquiritigenin micelle nanoparticles: formation, characterization, tissue distribution, pharmacokinetics and effects for ischemic stroke. *Int J Nanomed*. 2022;17:3655–3670. doi:10.2147/IJN.S368528
28. Li YX, Wang H-B, Jin J-B, et al. Advances in the research of nano delivery systems in ischemic stroke. *Front Bioeng Biotechnol*. 2022;10:984424. doi:10.3389/fbioe.2022.984424
29. Xiao Z, Li Y, Chen T, et al. A novel nitric oxide-driven nanomotor for synergistic treatment of ischaemic stroke: enhanced deep brain penetration and therapeutic efficacy. *Chem Eng J*. 2024;496:154205.
30. Tang L, Yin Y, Liu H, et al. Blood–brain barrier-penetrating and lesion-targeting nanoplatforms inspired by the pathophysiological features for synergistic ischemic stroke therapy. *Adv Mater*. 2024;36(21):2312897. doi:10.1002/adma.202312897

31. Liu L, Ma Z, Han Q, et al. Myricetin oligomer triggers multi-receptor mediated penetration and autophagic restoration of blood-brain barrier for ischemic stroke treatment. *ACS Nano*. 2024;18(14):9895–9916. doi:10.1021/acsnano.3c09532
32. You L, Wang J, Liu T, et al. Targeted brain delivery of rabies virus glycoprotein 29-modified deferoxamine-loaded nanoparticles reverses functional deficits in parkinsonian mice. *ACS Nano*. 2018;12(5):4123–4139. doi:10.1021/acsnano.7b08172
33. Lei L, Tu Q, Zhang X, et al. Stimulus-responsive curcumin-based polydopamine nanoparticles for targeting Parkinson's disease by modulating α-synuclein aggregation and reactive oxygen species. *Chem Eng J*. 2023;461:141606. doi:10.1016/j.cej.2023.141606
34. Bajgai B, Suri M, Singh H, et al. Naringin: a flavanone with a multifaceted target against sepsis-associated organ injuries. *Phytomedicine*. 2024;130:155707.
35. Wang L, Hu Y, Zhang H, et al. Neuroprotective effects of intraperitoneally injected Mg alloy extracts on middle cerebral artery occluded mouse with reperfusion injury. *J Magnes Alloys*. 2024. doi:10.1016/j.jma.2024.05.025
36. Hu J, Tao M, Sun F, et al. Multifunctional hydrogel based on dopamine-modified hyaluronic acid, gelatin and silver nanoparticles for promoting abdominal wall defect repair. *Int J Biol Macromol*. 2022;222:55–64. doi:10.1016/j.ijbiomac.2022.09.052
37. Zhou Z, Zhang X, Xu L, et al. A self-healing hydrogel based on crosslinked hyaluronic acid and chitosan to facilitate diabetic wound healing. *Int J Biol Macromol*. 2022;220:326–336. doi:10.1016/j.ijbiomac.2022.08.076
38. Li W, Shao C, Li C, et al. Metabolomics: a useful tool for ischemic stroke research. *J Pharm Anal*. 2023;13(9):968–983.
39. Poellmann MJ, Bu J, Hong S, et al. Would antioxidant-loaded nanoparticles present an effective treatment for ischemic stroke? *Nanomedicine*. 2018;13(18):2327–2340. doi:10.2217/nnm-2018-0084
40. Allen CL, Bayraktutan U. Oxidative stress and its role in the pathogenesis of ischaemic stroke. *Int J Stroke*. 2009;4(6):461–470. doi:10.1111/j.1747-4949.2009.00387.x
41. Liddelow SA, Guttenplan KA, Clarke LE, et al. Neurotoxic reactive astrocytes are induced by activated microglia. *Nature*. 2017;541(7638):481–487. doi:10.1038/nature21029
42. Liu Y, Zhang F, Long L, et al. Dual-function hydrogels with sequential release of GSK3β inhibitor and VEGF inhibit inflammation and promote angiogenesis after stroke. *Chem Eng J*. 2022;433:133671. doi:10.1016/j.cej.2021.133671
43. Zhao S-C, Ma L-S, Chu Z-H, et al. Regulation of microglial activation in stroke. *Acta Pharmacol Sin*. 2017;38(4):445–458. doi:10.1038/aps.2016.162